Fluid inclusion petrography

Article *in* Lithos · January 2001

DOI: 10.1016/S0024-4937(00)00037-2

2 authors:

Alfons van den Kerkhof
Georg-August-Universität Göttingen
103 PUBLICATIONS **2,311** CITATIONS

SEE PROFILE

Ulrich Hein
GZG Göttingen, Germany
16 PUBLICATIONS **682** CITATIONS

SEE PROFILE

ELSEVIER

Lithos 55 (2001) 27–47

LITHOS

www.elsevier.nl/locate/lithos

Fluid inclusion petrography

Alfons M. Van den Kerkhof [a,*], Ulrich F. Hein [b]

[a] *IGDL, University of Göttingen, Goldschmidstrasse 3, D 37077 Göttingen, Germany*
[b] *IMMR, Technical University of Clausthal, Adolph Roemerstrasse 2a, D 38678 Clausthal-Zellerfeld, Germany*

Received 15 September 1999; accepted 4 April 2000

Abstract

A procedure of fluid inclusion studies is proposed with emphasis on the criteria of selecting fluid inclusions for detailed (microthermometry and spectroscopic) analysis. An overview of descriptive and genetic classifications of fluid inclusions in single crystals and in massive rocks is given with the intention of further differentiating the commonly used terms 'primary' and 'secondary' fluid inclusions. Some principles of fluid inclusion modification are explained. Cathodoluminescence (CL) studies of quartz with the optical high-power CL-microscope and the electron microprobe provided with a CL detector are an important help in 'fluid petrography'. CL textures are subdivided in primary, growth textures and a wide variety of secondary microtextures, which are in part induced by fluid inclusions. The latter is grouped in textures indicative of local lower crystal order (increasing defect structures) and microtextures indicative of local quartz healing (reduction of the defect structures). Microtextures showing the genetic relationship between fluid inclusions and the host mineral provide information about the possible post-entrapment changes of fluid inclusions and therewith testify their geological relevance.

Keywords: Fluid inclusions; Petrography; Fluid inclusion classifications; Decrepitation; Cathodoluminescence; Quartz

1. Introduction

Petrographic microscopy of a rock sample is the first and at the same time essential step of any fluid inclusion study. A proper interpretation of fluid inclusions can be made only when textural relationships between fluid inclusions and the host mineral are considered. Missing the right context, even huge numbers of microthermometry and analytical data do not contribute much in revealing the rock-forming conditions. Ideally, a fluid inclusion study should be integrated in petrology, including rock and mineral analysis, and can be successful only when sufficient time (and this means, in many cases, also money) is invested: as a general indication, a study period of some months is more realistic than some weeks. A fluid inclusion study done to obtain just some homogenization temperatures in order to check a geological thermometer or any other geological interpretations mostly ends in disappointment. Fluid inclusions should not be considered as a study method, but as an integrate part of the rock and worth studying as such. Like the minerals, fluid inclusions do not tell us about one particular episode of the rock-forming processes, but generally about different stages of the rock evolution. When properly interpreted, fluid inclusions provide information,

* Corresponding author.
E-mail address: akerkho@gwdg.de (A.M. Van den Kerkhof).

0024-4937/01/$ - see front matter
PII: S0024-4937(00)00037-2

which cannot be obtained otherwise: they are the only *direct* evidence for the role of the fluid during geological processes. In addition to petrological microscopy, the application of cathodoluminescence (CL) microscopy is highly powerful for the interpretation of fluid inclusion-related microtextures. An overview of CL applications to fluid inclusion studies is given in the last part of this paper. The interpretation of fluid inclusions in rocks may request also some knowledge of experimental studies on the behavior of fluid inclusions on changing PT and indicative of the dynamics of fluid inclusion formation and re-equilibration. Any fluid inclusion study, however, needs a clear strategy made at an early stage of investigation, mostly by an inventory study of the minerals and fluid inclusion-related textures.

2. The fluid inclusion study procedure

A rock may contain millions of fluid inclusions per cubic centimeter and consequently, an intelligent selection of the fluid inclusions for detailed analysis is indispensable. However, this step may already highly effect the final result. The first selection already starts during rock sampling in the field. The variation of the different lithologies within one outcrop should be documented and the position of the sample in the rock sequence specified. Even within the same lithology, fluid inclusions may show considerable variation in composition and density and it is advised to take at least two or three samples from the same outcrop in order to get an overall impression of the fluid inclusion variation. It is self-evident that for special studies (e.g. zoned veins), a systematic sampling of many more samples from one locality may be necessary. A study of the enderbitic granulites in Bamble, Norway (Van den Kerkhof et al., 1994) showed that carbonic fluid inclusions in quartz samples taken only some meters apart from apparently homogeneous rocks may have very different densities. These fluid inclusions were subject of different re-equilibration rates controlled by local variations of deformation. In these rocks, only one fluid inclusion out of randomly selected 800 inclusions appeared as possibly trapped at granulite-facies conditions, whereas other inclusions had been modified during subsequent stages of uplift and retrograde metamorphism (Vityk and Bodnar, 1995b).

Sample preparation for fluid inclusion studies is done by making doubly polished sections of 100–300 μm thickness. Ideally, a normal polished thin section is made from the *same* sample for microscopic studies, electron microprobe analysis (mineral thermobarometry), and eventually, also for CL microscopy.

Selection and grouping of fluid inclusions should be done prior to any other analysis (microthermometry, Raman analysis, etc.). Any grouping done afterwards based on fluid inclusion compositions and densities (as obtained from scatter plots of microthermometry data) and by using these groups for genetic interpretation in many cases appeared to be useless. Particularly, the interpretation of histogram presentations of microthermometry data should be done with greatest care. Too many times the simple correlation of 'temperature frequency maxima' with one of the rock's main metamorphic events has led to erroneous conclusions. Like the rock-forming minerals, fluid inclusions found in rocks at the earth's surface are the result of geological processes at high-temperatures as well as re-equilibration during uplift. Besides, re-equilibration of fluid inclusions is partly controlled by crystal dynamics (like 'necking down') which are not directly related to geological events like metamorphism or deformation. The scale on which fluid inclusion-forming processes act may vary from a few microns (e.g. diffusion during crystal growth, re-crystallization) up to several tens of kilometers and more in the case of orogenic events and related fluid migration (Bethke and Marshak, 1990). Not all fluid-inclusion related textures are formed by large-scale geological processes, but they are in part controlled by the crystal dynamics of the host mineral and by physico-chemical processes controlled by the crystal–fluid interface. Fluid inclusions should not be considered as simple cavities filled with fluid, but as an integrative system, which also comprises a part of the host mineral. The quartz immediately surrounding a fluid inclusion may show deviant concentrations of defect structures (higher or lower) compared to the overall quartz host mineral. Microtextures like dislocations, microcracks, and secondary (re-crystallized) quartz are often found around fluid inclusions (Fig. 1; see also Viti and

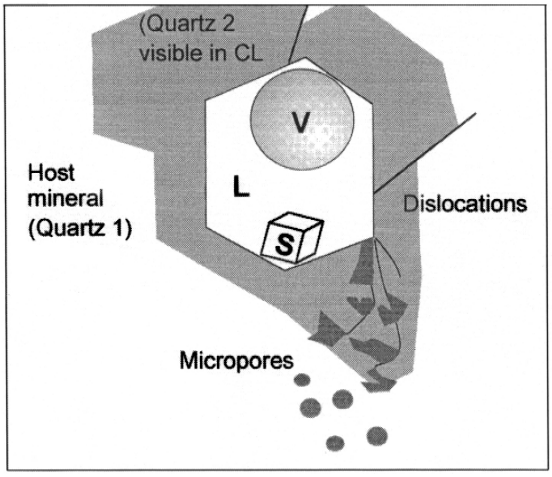

Fig. 1. The integrative fluid inclusion–mineral system. The most important elements in and around a fluid inclusion in quartz are schematically drawn. Fluid inclusions may be surrounded by pure secondary quartz as a result of partial quartz recovery (here: re-crystallization and diffusion). The overall host and secondary quartz generations can be distinguished by CL. Structural defects like dislocations induced by the fluid inclusion are frequently found and may function as the pathways for water leakage.

Frezzotti, 2001). These textures can be made visible by CL (see later in this paper) and are highly useful in order to draw conclusions about the interaction processes between a fluid inclusion and its host mineral. Fluid inclusions can be considered as huge defects of the crystal lattice and are always more or less in a state of non-equilibrium and therefore, constantly tend to interact with the host mineral.

The *selection of fluid inclusions* for microthermometry measurements is not always simple and a certain subjectivity cannot be avoided. Particularly in metamorphic rocks, fluid inclusions in many cases look chaotic at first sight and any systematic study seems almost hopeless. We need selection criteria in order to choose the fluid inclusions for further analysis. Certainly, any selection is liable to subjective criteria and finding 'representative' fluid inclusions an impossible task. However, more importantly, we should answer the question which fluid inclusions are representative for what? As a general rule, a homogeneous fluid trapped at the same pressure and temperature conditions *must* result in fluid inclusions which are *identical* in composition and density. As a general rule, only *interpretable* fluid inclusions should be measured; collecting astronomical numbers of fluid inclusion data without the necessary textural information, in most cases, is a waste of time. Fluid inclusions formed at more or less the same stage of rock evolution are sometimes designated as belonging to the same fluid inclusion 'generation'. Touret (2001), in this volume, uses 'groups of simultaneous inclusions' and Goldstein (2001) prefers the term 'fluid inclusion association'. These differences in the nomenclature, however, are not essential and re-defining the old terms may be as worthy as finding alternatives for unclear or sometimes misused 'old' ones. Most important is to group the fluid inclusions in a rational way, depending on the study case, and therewith indicate their geological relevance. Once distinguished on a textural basis, one must stick to this classification and better define each of the groups during the subsequent analytical procedure. The properties of each group should be further constrained and not differentiated.

A general indication about the number of fluid inclusions to be analyzed cannot be made. Only a few measurements are sufficient to characterize apparently similar fluid inclusions, which belong to the same generation. On the other hand, we may apply statistics (with greatest care) to the data obtained from fluid inclusions modified to a different extent, however, by the same process; for these inclusions a number of 30–100 per sample is commonly used.

3. Descriptive classification of fluid inclusions

Fluid inclusions can be described by visual parameters like size, shape, color, refractive index and particularly by the phases present at room temperature. The term 'fluid inclusions' may be somewhat captious since at room temperature more than one phase is normally present, i.e. liquid (L), gas or vapor (V), eventually together with one or more solid phases (S), which may be accidentally trapped or formed as a daughter phase during cooling (Fig. 2). In magmatic rocks also, glass (G) is commonly found as inclusions together with one or more 'volatile' phases. The interpretation of glass inclusions being subject of extensive studies requires specific approach applied to magmatic processes and is not considered in this paper.

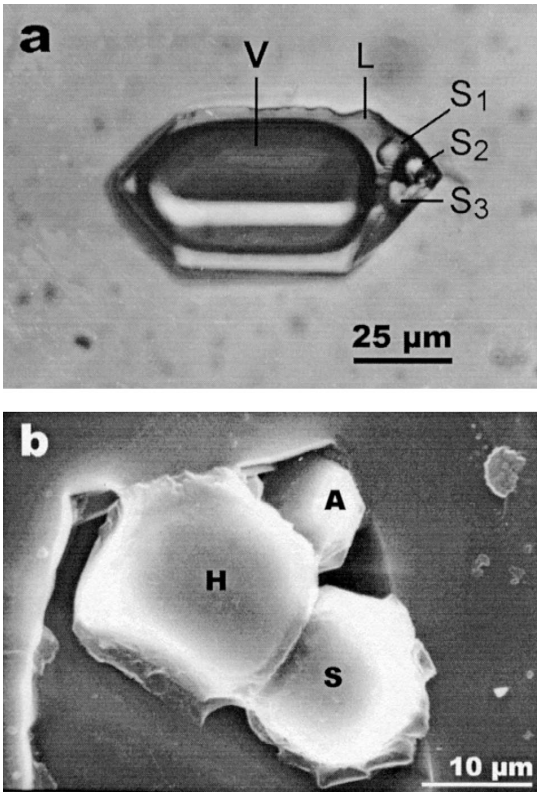

Fig. 2. (a) Multi-phase fluid inclusion in smoky quartz containing a large bubble (V) of CO_2, saturated salt solution (L) and various daughter phases denoted by S_1, S_2, and S_3. (b) SEM image of an opened fluid inclusion containing three daughter phases (H = halite; S = sylvite; and A = arcanite) from the same location. Samples from Gakara, Burundi (Hein, 1998).

The *host mineral* provides important information about the forming conditions, not only because minerals may crystallize and trap fluids at different episodes, but also because fluid inclusions are better preserved in some minerals than in others. Fluid inclusions may occur in almost all minerals, but in practice, more than 90% of the fluid inclusions studies consider fluid inclusions in quartz. The absence of cleavage and the ability of easy re-crystallization make quartz a highly suitable medium to preserve fluid inclusions. In some cases, however, fluid inclusions are well preserved in garnet, olivine, pyroxene, cordierite, feldspar, carbonate, scapolite, fluorite, halite, etc. Once formed, fluid inclusions in these minerals represent different stages of rock formation. Notably, garnet and to a lesser extent, also plagioclase, are more resistant to deformation and may preserve fluids dating from the earliest stage of metamorphism (e.g. Coolen, 1982; Herms and Schenk, 1998).

Although the *size* of fluid inclusions shows extreme variation from < 1 μm up to sizes observable in the hand specimen, most visible fluid inclusions fall in the range, 5 to 20 μm. A significant fraction of fluid inclusions $\ll 1$ μm is observable only by TEM (Viti and Frezzotti, 2001). A severe problem in estimating the size (volume) of fluid inclusions is their irregular shape, normally observed in two dimensions. Advanced techniques like the spindle stage allow three-dimensional characterization of the fluid inclusions (Anderson and Bodnar, 1993). Bodnar (1983) described a method to calculate more precisely fluid inclusion volumes from the bubble diameter and the homogenization temperature, for fluid compositions defined by the freezing temperature.

The fluid inclusion cavity tends to form crystal phases by re-crystallization and/or dissolution–precipitation. The result is the so-called 'negative crystal shape', typical for many natural fluid inclusions (Fig. 3). By reducing the surface energy, regularly shaped inclusions represent the most stable state. Using the 'negative crystal shape' as one criterion for primary (early) entrapment (Roedder, 1984) should be done with greatest care as re-equilibrated inclusions with the same characteristics have also been found in many cases.

With exceptions (some organic fluids, see Munz, 2001), fluid inclusions are normally colorless in thin section. However, the difference of *refractive index* with the host mineral may, depending on the optics (position of the condenser and the diaphragm), cause dark, grayish or pinkish colors. Actually, we are able to observe fluid inclusions because the refractive indices for fluid inclusion and host mineral are normally different. By optical observation, we may distinguish the generally higher density aqueous inclusions (refractive index 1.32–1.33 and showing as bright inclusions) from the lower density gas inclusions. Liquid CO_2 has a refractive index of about 1.195, gaseous CO_2 a much lower refractive index and appears dark.

The number and type of *phases present at room temperature* is one of the most useful and widely

applied criterion to describe fluid inclusions. The content of a fluid inclusion may be given by the phases and number of phases as a subscript. For example: an inclusion containing liquid (L), vapor (V), and two salt crystals (S_1 and S_2) can be typified as LVS_1S_2. The relative volumes of the phases can be estimated by using tables proposed by Roedder (1984) and Shepherd et al. (1985).

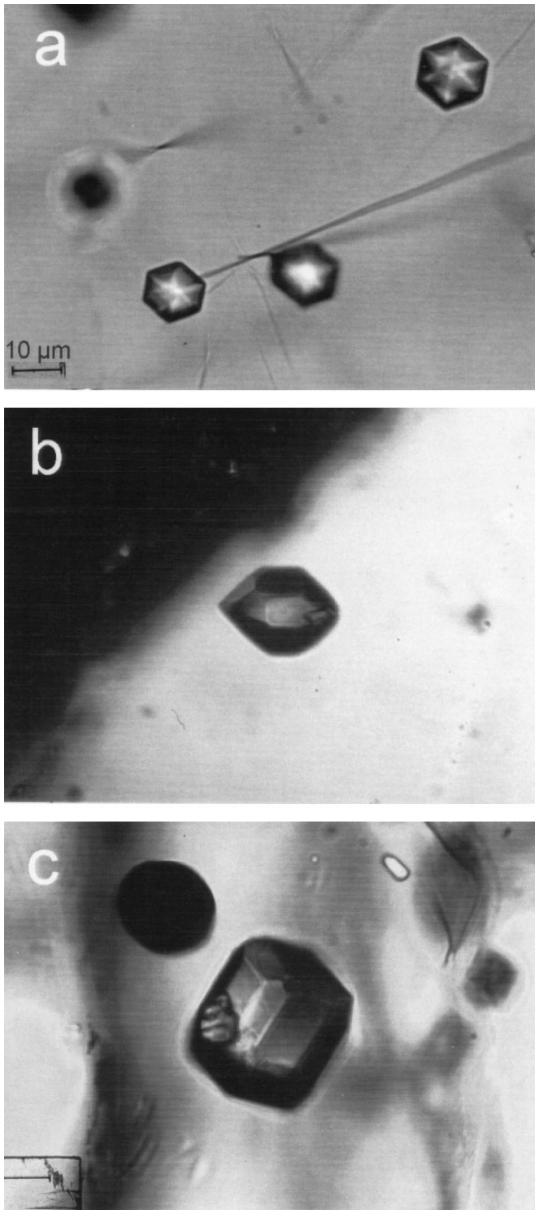

Fig. 3. Fluid inclusions showing 'negative' crystal shape (a) in quartz from the Furua Granulite Complex, Tanzania (sample: Coolen, 1982). High-density hexagonal $CO_2 \pm N_2$ fluid inclusions (molar volume 35 cm^3/mol) are all arranged perpendicular to the *c*-axis of the host quartz; (b) in hydrothermal quartz from Gakara, Burundi (Hein, 1998) liquid CO_2 fluid inclusions are observed here parallel to the *c*-axis, and (c) in garnet from Rundvagshetta, Lützow-Holm Bay, Antarctica (Kooi et al., 1998). The fluid inclusion contains a CO_2–N_2 mixture (molar volume 42 cm^3/mol) and has a combined rhombic dodecahedron–ikoso–tetrahedron morphology, typical for garnet. A carbonate daughter crystal can be observed on the lower left wall of the fluid inclusion cavity (photos a, b, and c are taken with the same magnification).

In many fluid inclusions, solid daughter phases can be found. These phases nucleate when fluid inclusions become oversaturated during cooling. The daughter phase at any temperature below the dissolution temperature is in equilibrium with the saturated fluid (normally, but not necessarily water). For example, the solution in a brine inclusion containing halite at room temperature (and no other salts present) has a salt concentration of about 27 wt.%. Table 1 shows the optical properties of solid phases in fluid inclusions in order of increasing refractive index. Also indicated are the refractive indices of some important host minerals. The refractive indices of quartz and halite are about the same and as a consequence, halite crystals nucleated on the inclusion wall may be easily overlooked.

4. Genetic classification of fluid inclusions (mechanisms of formation)

The spatial relationships of fluid inclusions provide information about the time of formation with regard to the host mineral. In describing fluid inclusions, we recommend making free-hand sketches during microscopy observations. By making photographs, not only much information is lost because of the impossibility of focussing fluid inclusions at different levels in the sample, but the textural relation between fluid inclusion and host mineral cannot be adequately shown. By making drawings, the inclusionist is forced to interpret his/her observations already during the earliest stage of investigation. As

Table 1
Optical properties of solid phases in fluid inclusions in order of increasing refractive index (literature compilation)

Name	Composition	Refractive index	Birefringence	Crystal system	Habit	Comments
Liquid carbon dioxide	CO_2 (liquid)	1.195				
Carbon dioxide	CO_2 (solid)	?		C	translucent, microcrystalline aggregates	$T < -56.6$°C; usually forms a single mass; euhedral crystals can be formed in liquid CH_4–CO_2
Ice	H_2O	1.31	negligible	H	rounded plates or globules	anisotropic but appears isotropic; Tm < 0°C; sometimes yellowish appearance
Water	H_2O	1.32–1.33				
CO_2-clathrate (gas hydrate)	$CO_2 \cdot 5\ 3/4H_2O$	~	negligible		rhombic or rounded grains	Tm = about 6°C; colorless, RI very close to water; RI very close to H_2O and therefore difficult to recognize
Villiaumite	NaF	1.33	isotropic	C	cubes	sometimes yellow/ pinkish pleochroism
Cryolite	Na_3AlF_6	1.34	negligible	M		alkaline rocks
Elpasolite	K_2NaAlF_6	1.37	isotropic	C		topase from Volynia USSR
Mirabilite (Glauber's salt)	$Na_2SO_4 \cdot 10H_2O$	1.39–1.40	negligible	M	prismatic, acicular	
Hydrohalite	$NaCl \cdot 2H_2O$	~ 1.41	negligible	M	tiny grains giving a speckled appearance	high relief relative to ice; colorless; Tm (incongruent) = + 0.1°C
Natron (soda)	$Na_2CO_3 \cdot 10H_2O$	1.40–1.44	low	M	platy crystals	Tm (incongruent) = + 32°C
Fluorite	CaF_2	1.43	isotropic	C	cubes	rarely octahedral, fluorescent
Hexahydrite	$MgSO_4 \cdot 6H_2O$	1.45	low	M	fibrous, tabular	
Trona	$Na_3H(CO_3)_2 \cdot 2H_2O$	1.41–1.54	moderate	M	fibrous, acicular	
Nahcolite	$NaHCO_3$	1.37–1.58	very high	M	tabular	commonly twinned; marked relief changes on rotation in pol. light; carbonic fluids in granulite facies
Alum	$(Na,K)Al(SO_4)_2 \cdot 12H_2O$	1.44–1.46	isotropic	C		
Sulfohalite	$Na_6(SO_4)_2ClF$	1.45	isotropic	C		
Thermonatrite	$Na_2CO_3 \cdot H_2O$	1.42–1.52	moderate	O		
Borax	$Na_2(B_4O_5(OH)_4) \cdot 8H_2O$	1.45–1.47	low	M		
Gaylussite	$Na_2Ca(CO_3)_2 \cdot 5H_2O$	1.44–1.52	moderate	M	elongated or flattened crystals	
Epsomite	$MgSO_4 \cdot 7H_2O$	1.43–1.46	low	O(T)	acicular	
Alunogen	$Al_2(SO_4)_3 \cdot 18H_2O$	1.46–1.48	low	T(H)	fibrous	
Thenardite	Na_2SO_4	1.46–1.48	low	O	bipyramidal or tabular	cf. gypsum

Carnalite	$KMgCl_3 \cdot 6H_2O$	1.47–1.49	low	O(H)	tabular	
Pickeringite (Mg)-halotrichite (Fe″)	$(Mg,Fe'')Al_2(SO_4)_4 \cdot 22H_2O$	mean 1.48	very low	M	acicular, radiated aggregates	
Sylvite	KCl	1.49	isotropic	C	cubes	often rounded cube edges, solubility at higher temperature; increases more rapidly compared to halite
Burkeite	$Na_6CO_3(SO_4)_2$	mean 1.49	moderate	O		
Arcanite	K_2SO_4	1.49–1.50	low	O	massive, tabular	rarely octahedral crystals
Pseudo-bischofite	$MgCl_2 \cdot 6H_2O$	1.49–1.50	low to moderate	M		
(hydro-)Bischofite	$MgCl_2 \cdot 12H_2O$	1.50–1.53	negligible	M	like hydrohalite	identification difficult; colorless
Wavellite	$Al_3(PO_4)_2(F,OH)_3 \cdot 5H_2O$	1.52–1.55	low	O	radiated aggregates, globules	
Gypsum	$CaSO_4 \cdot 2H_2O$	1.52–1.53	very low	M	tabular, prismatic, fibrous	
Hydromagnesite	$Mg_5(CO_3)_4(OH)_2 \cdot 4H_2O$	1.52–1.54	low	M(O)	acicular crystals or lamellae	
Hydroboracite	$CaMg[B_3O_4(OH)_3]_2 \cdot 3H_2O$	mean 1.52	moderate	M		associated with gypsum
Dawsonite	$NaAl(CO_3)(OH)_2$	1.47–1.60	moderate	O	fibrous bundles, aggregates	frequent in alpine fissures
Halite	NaCl	1.54	isotropic	C	cubes	rarely octahedral, same refractive index as quartz
Fe-chlorides	$FeCl_n$	various	moderate to high	(T) various	tabular, often rhombic or hexagonal	commonly light green
Quartz	SiO_2	1.54–1.55	low			
Antarcticite	$CaCl_2 \cdot 6H_2O$	1.49–1.55	low/negligible	T	like hydrohalite but occasionally rounded crystals	
Micas	various	1.56–1.60	low to moderate	M	platy	extremely thin plates
Strontianite	$SrCO_3$	1.52–1.67	high	O	acicular, pseudohexagonal	
Anhydrite	$CaSO_4$	1.57–1.61	low	O	prismatic	associated with gypsum
Aragonite	$CaCO_3$	1.53–1.69	high	O	prismatic, acicular	
Whewellite	$CaC_2O_4 \cdot H_2O$	1.49–1.65	very high	M	prisms	uranium vein deposits
Ca,Mg carbonate	$(Ca,Mg)CO_3$	1.49–1.66	very high	T	rhombohedral	high relief; marked changes in relief on rotation in polarized light
Barite	$BaSO_4$	1.64–1.65	low	O	tabular	
Apatite	$Ca_5(PO_4)_3(F,OH,Cl)$	1.63–1.67	low	H	hexagonal crystals	
Hematite	Fe_2O_3	(2.9–3.2)		T	hexagonal plates	distinctive red/brown plates
Sulfides	various	–		various	euhedral grains	identification sometimes possible in reflective light
Graphite	C	–		H	mostly amorphous	euhedral (platy) crystals rare; highly Raman active

C: cubic, M: monoclinic, O: orthorhombic, T: triclinic, Q: tetragonal and H: hexagonal.

a matter of fact, interpretations from purely descriptive, objective terms are impossible.

Primary fluid inclusions by definition are trapped during crystal growth, whereas secondary fluid inclusions can be trapped at any time after the growth of the host crystal. Fluid inclusions in microcracks formed *during* crystal growth are referred to as 'pseudosecondary'. The 'primary–secondary' terminology is essentially applied to non-deformed euhedral or subhedral crystals (Fig. 4). Diagnostic criteria for classifying fluid inclusions as primary or secondary have been proposed by Roedder (1979). Examples of primary inclusions are given in Fig. 5a for single crystals, in part, in respect to growth zonation (Fig. 5b). When applied to massive rocks, as done in the past by many fluid inclusionists, the terms pri-

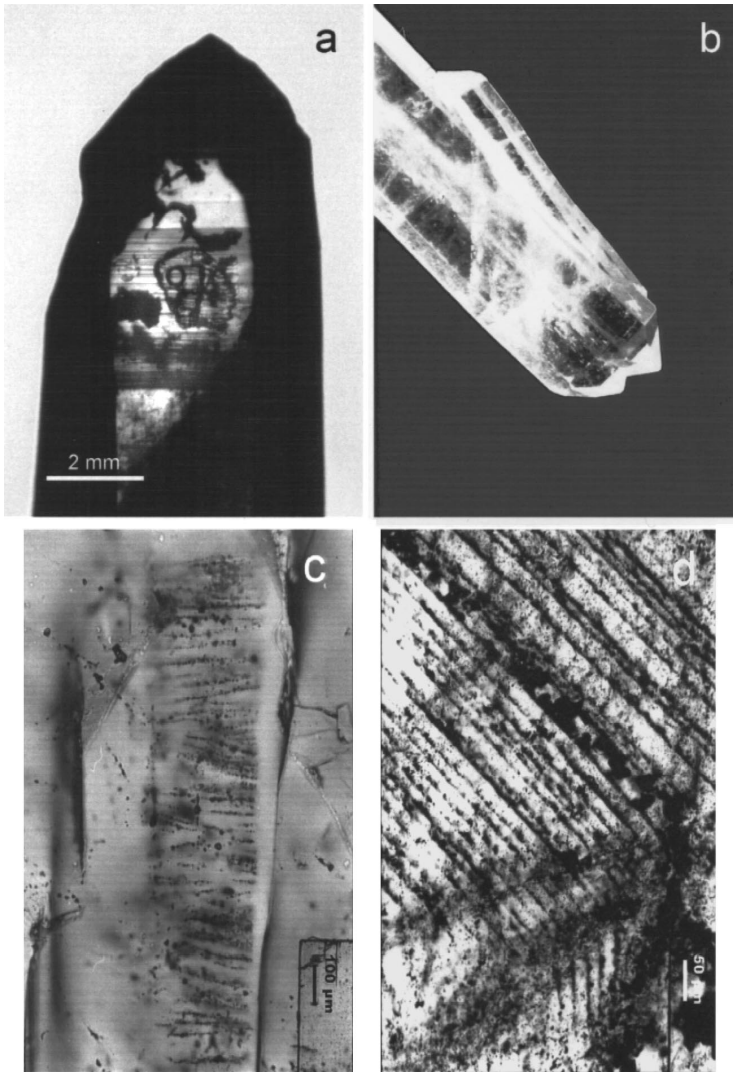

Fig. 4. Examples of primary fluid inclusions: (a) quartz crystal from Osilo, Sardegna, Italy, containing a large (2 mm diameter) aqueous inclusion. (b) Striped quartz from the Ramsbeck mine (Rhenish Massif, Germany); the central stripe consists of primary inclusions, which are orientated perpendicular to the growth direction of the crystal. (c) Fibrous quartz showing primary fluid inclusions trapped along trails during crack-seal growth. (d) Primary aqueous fluid inclusions decorating growth zones of hydrothermal quartz from Holzappel (Rhenish Massif, Germany).

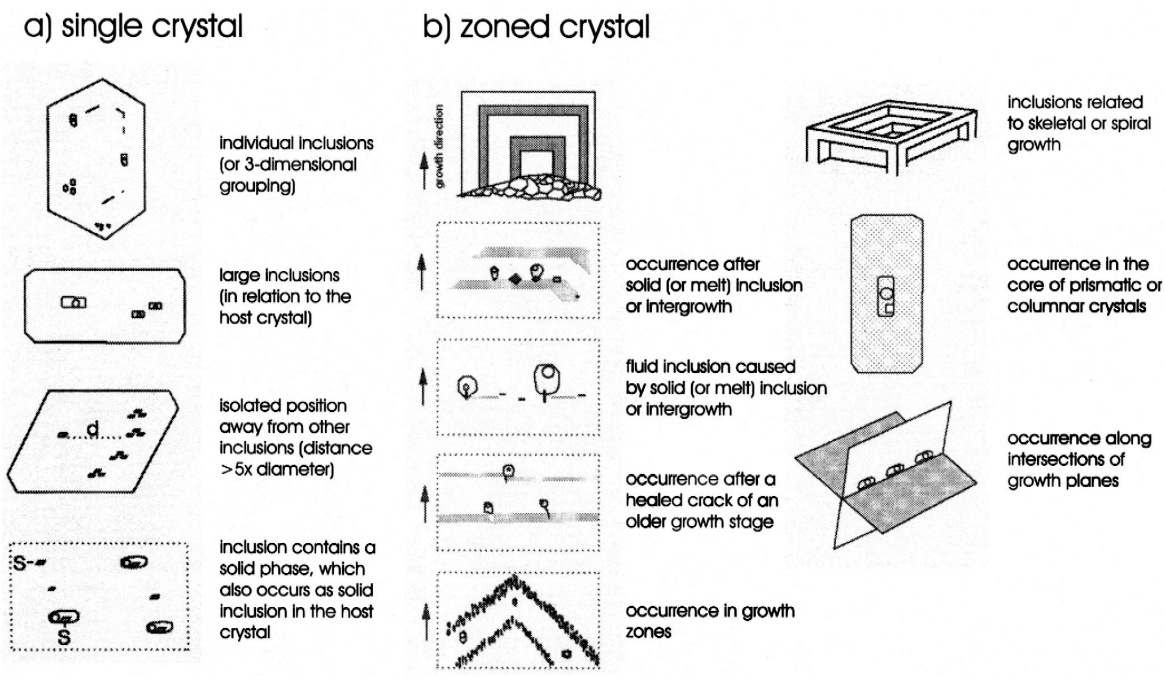

Fig. 5. (a) Diagnostic criteria for classifying fluid inclusions as primary (drawn after Roedder, 1979). (b) Different occurrences of primary fluid inclusions in relation to growth zonation (compilation from the literature).

mary and secondary may be misleading as primarily grown minerals generally are not preserved. In this case, the terms 'early' vs. 'late' better characterize the relative chronology of trapping. In spite of the difficulties of applying the 'simple' primary–secondary terminology to complex natural samples, these terms appeared to be highly useful as they imply important differences of the fluid regime: the formation of primary inclusions requires that the rock system was supersaturated with respect to the host mineral, whereas fractures will heal and trap secondary inclusion even if the bulk fluid (outside the fracture) was undersaturated with respect to the host crystal (L. Diamond, personal communication).

In *massive rocks*, fluid inclusions can be principally subdivided in (a) isolated fluid inclusions, (b) inclusions in clusters, and (c) fluid inclusions in trails, essentially representing healed microcracks. The trails can be classified according to the terminology proposed by Simmons and Richter (1976) and Kranz (1983) (Fig. 6).

(a) Transgranular inclusions form in healed microcracks cross-cutting grain boundaries (Fig. 6a).

(b) Intergranular inclusions decorating grain boundaries may be related to two processes: (1) healing of extensional grain boundary cracks and (2) fluid collection during grain boundary migration. These textures are particularly common in rocks which underwent intensive dynamic re-crystallization (Fig. 6a).

(c) When considering fluid inclusions in textural relationship with different mineral phases, the terms 'interphase' for fluid inclusions formed along phase boundaries and 'transphase' for fluid inclusions in trails cross-cutting different mineral phases can be applied (Fig. 6a).

(d) Intragranular inclusions occur within single grains and do not cross-cut grain boundaries. They may be interpreted as the result of fluid trapping along surfaces showing preferent crystallographic orientation. These surfaces may be cleavage planes, deformation lamellae, deformation bands, subgrain boundaries or twinning lamellae (Fig. 6b).

Intersection of trails of different fluid inclusions give rise to a number of features which can be used for establishing the fluid chronology (Touret, 1981).

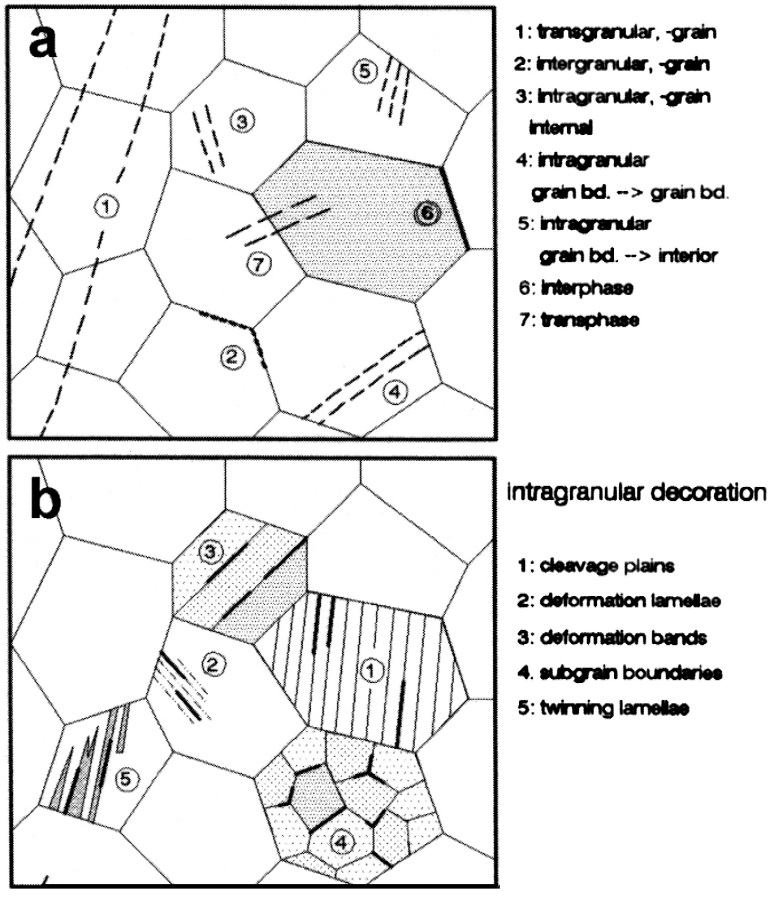

Fig. 6. (a) Trail terminology (Vollbrecht, 1989) composed after Simmons and Richter (1976) and Kranz (1983). A main distinction is made between transgranular, intergranular, and intragranular inclusions. (b) The intragranular fluid inclusions may decorate different internal grain textures and are accordingly subdivided.

A common phenomenon is the refilling of fluid inclusion in the region of intersection.

Trapping of a homogeneous fluid at one particular episode of the rock evolution results in fluid inclusions which are essentially identical in appearance, composition, and density (Figs. 7a and 8). After cooling, phase separation should result in fluid inclusions of the same degree of fill, except in the case where a bubble hampers to form due to metastability. The latter is common for high-density aqueous inclusions with expected homogenization temperatures below about 150°C. During subsequent cooling after first trapping, shrinkage of the fluid phase compared to the almost unchanged volume of the host mineral normally results in bubble formation ($L \rightarrow LV$). Sometimes, liquids separate ($L \rightarrow L_1L_2$) or daughter crystals form ($L \rightarrow LS$). Combinations of these phase changes normally occur during cooling (Fig. 7). Trapping of immiscible liquids (heterogeneous trapping) or during boiling may result in fluid inclusions of variable composition and density (Figs. 7b and 9).

5. Decrepitation and modification of fluid inclusions

The term decrepitation refers to the leakage or partial leakage of the fluid by the formation of microfractures as a result of fluid overpressure, i.e.

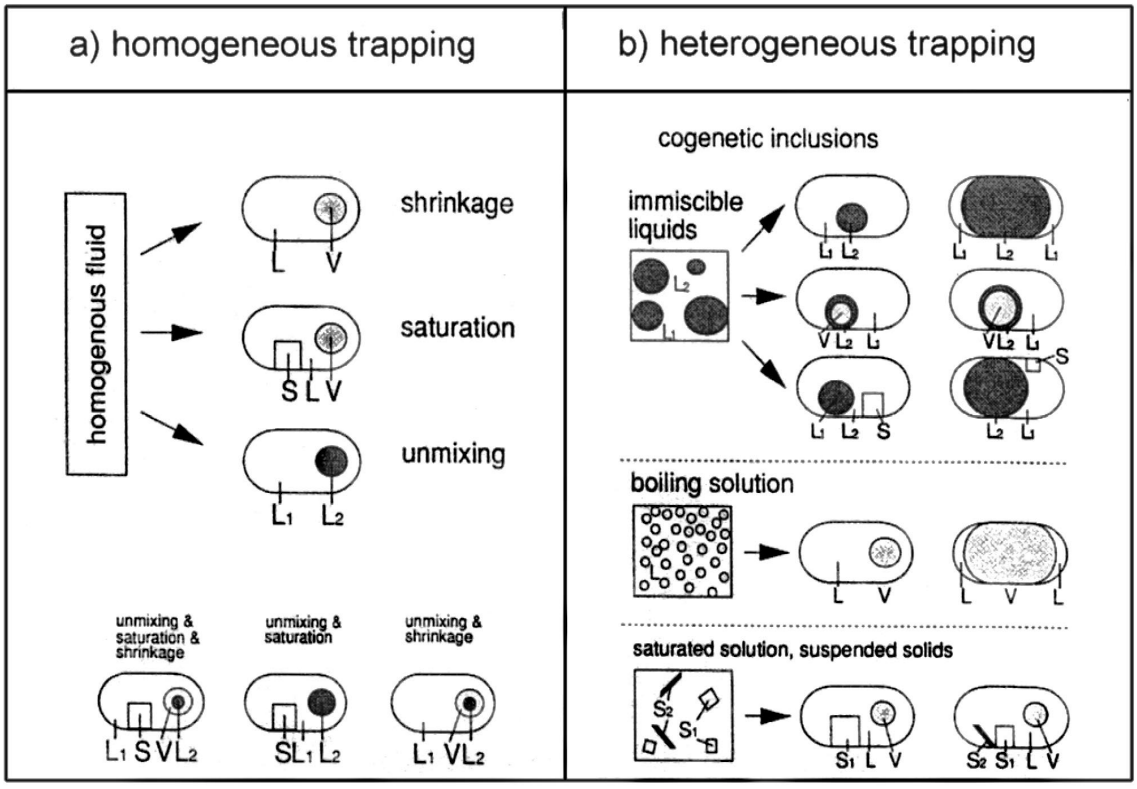

Fig. 7. (a) Homogeneous trapping of fluids. At room temperature (after cooling), phase separation may result from shrinkage, saturation or unmixing of the original homogeneous fluid. (b) Heterogeneous trapping of fluids. Fluid inclusions of variable composition and phase ratio are trapped at the same time.

the pressure gradient between fluid pressure and confining pressure. Decrepitation can be achieved during heating experiments notably during microthermometry measurements. The temperature of decrepitation (Td, Roedder, 1984) defines the destruction of the inclusion on heating and is normally higher than the homogenization temperature (Th). As the isochores for aqueous systems show a rapid pressure increase towards higher temperatures, decrepitation normally takes place at some degrees above Th. On the contrary, the isochores of gas-rich systems are flat and consequently, gas inclusions are preserved better. Also, the properties of the host mineral (hardness, cleavage) strongly effect the preservation of fluid inclusions, e.g. quartz may preserve fluid inclusions of much higher pressure compared to minerals with much better cleavage like calcite or fluorite.

The processes controlling the changes of fluid inclusions after first entrapment comprise more than mechanical fracturing alone and also include stretching, water diffusion through dislocations (hydrolytic weakening), the formation of secondary quartz by dissolution–precipitation, and by re-crystallization. Although the term ‘decrepitation’ for any process responsible for post-entrapment changes of fluid inclusions finds wide application in the literature, modification or re-equilibration are considered better terms to describe the various changes of fluid inclusions on changing the pressure and temperature. The term decrepitation may be preserved for the physical loss of material from fluid inclusions during experimental heating. ‘Stretching’ describes volume changes without the loss of material.

Most of the knowledge on fluid inclusion decrepitation is based on the experimental studies of Sterner

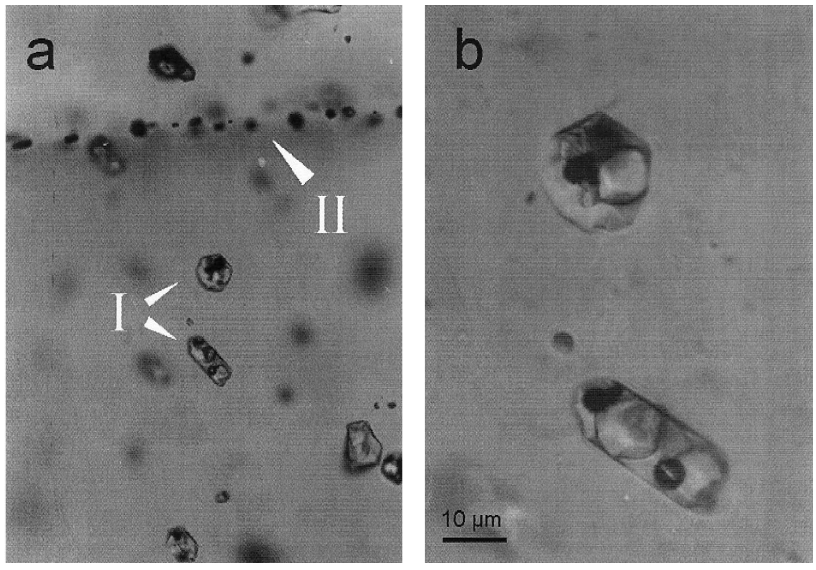

Fig. 8. (a) Two generations of fluid inclusions (I and II) in quartz: the earlier generation contains the same number of phases (including three salts and one opaque crystal) and the same phase ratios. The later generation is made up by CO_2 inclusions of the same density trapped along a healed fracture. (b) Detail of (a). The daughter crystals were identified by Raman microspectrometry and by electron microprobe as halite, sylvite, and arcanite (see also Fig. 2 for further detail). Sample from Gakara, Burundi (Hein, 1998).

and Bodnar (1989), Vityk and Bodnar (1995a), Bakker and Jansen (1994), and others. One of the aims of these experiments is to correlate fluid and tectonic evolutions in the rock. It was recognized that fluid inclusion morphologies are indicative of explosion or implosion events (Vityk and Bodnar, 1995a). The textures found by re-equilibration experiments in autoclaves are in good agreement with observations in natural quartz.

One of the most important parameters inducing fluid inclusion modification is the gradient (overpressure or underpressure) between fluid inclusions internal pressure and the external confining pressure (in geological terms, normally, the lithostatic pressure) and the fluid inclusion size. Fig. 10 shows the three principle regimes of fluid inclusion modification: isothermal decompression (ITD), isobaric cooling (IBC) and isochoric cooling (ICC). Once trapped and closed, the pressure in any fluid inclusion is defined by the isochore valid for the fluid density and composition at the time of trapping. Any uplift path, which does not exactly follow the isochore will cause a pressure difference between the fluid inclusion and its surrounding. If the pressure difference exceeds a given value, the fluid inclusion collapses and the fluid density is adjusted to the ambient pressure and temperature. In the case of isothermal uplift, fluid inclusions have higher pressure than the ambient pressure. The maximum overpressure in quartz has been experimentally determined (Bodnar et al., 1989) as 1–4 kbar for 1–20 μm size fluid inclusions (with the smallest inclusions most resistant to modification). The inclusion will expand or lose a part of its content by partial leakage through microfissures and dislocations. This process which is not yet completely understood in detail is referred to as 'explosion–decrepitation'. Interesting and yet unexplained are the many exceptions of fluid inclusion preservation, at much higher pressures than shown by the 'mean' experimental results. These inclusions are found in the experiments (e.g. Vityk and Bodnar, 1995b) as well as in natural rocks, e.g. many CO_2 inclusions in olivine nodules must have been able to withstand more than the pressure limit found by experiment, given the wide divergence of isochores and the essentially isothermal decompression paths.

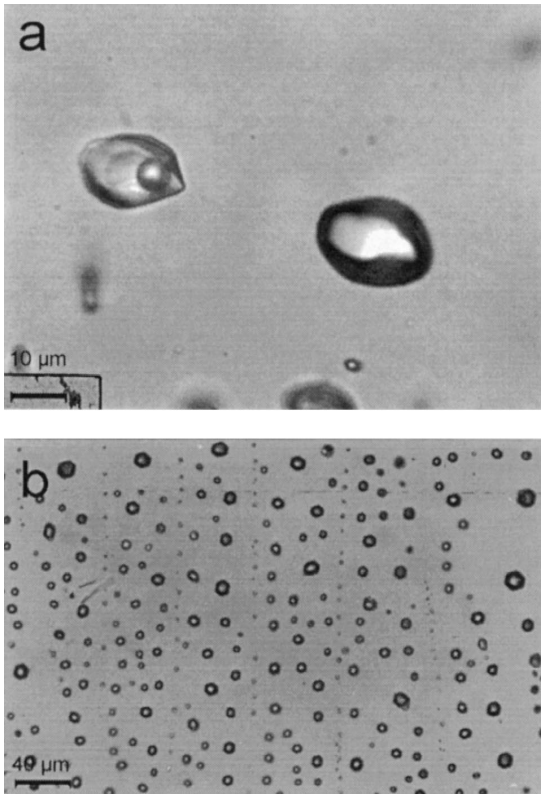

Fig. 9. Heterogeneously trapped fluid inclusions. (a) Co-genetic pair of fluid inclusions containing (left) water with a methane bubble and (right) liquid methane and an invisible rim of water along the cavity wall. Sample from Armsfeld (Kellerwald, Germany) (Hein et al., 1994a,b). (b) Healed fracture in smoky quartz containing co-genetic CO_2-rich inclusions (equally distributed in the plane and showing negative crystal shape) and tiny brine inclusions (arranged along trails on regular distance).

In the case of isobaric cooling, the pressure in the inclusion becomes lower than its surrounding. Fluid inclusions in quartz are found to collapse ('implosion–decrepitation') for fluid underpressure > 2 kbar (Sterner and Bodnar, 1989).

Textural evidence for the crystallization of newly-formed quartz in decrepitated and leaked inclusions has been described by Voznyak and Kalyuzhniy (1976) in quartz from Volyn (Russia) and later also by Hurai and Horn (1992) in quartz samples from the Western Carpathians (Slovakia) and in gold-bearing quartz veins from Burundi (Hein et al., 1994a,b) (Fig. 11). In these inclusions, the loss of fluid volume is compensated by quartz growth in the inclusion cavity. These observations show that the diffusion of water out of fluid inclusions is mainly controlled by fluid–quartz interface effects and may induce other secondary effects like re-crystallization. From the orientation of the halo planes around similar inclusions in granite, Audétat and Günther (1999) assumed a modification mechanism induced by asymmetrical stress distribution around the inclusion and that fluid overpressure does not play a role. Partial leakage may considerably influence the fluid composition: water is much more mobile due to the higher polarity of the water molecules compared to gas. Therefore, modified inclusions preferentially lose water and are enriched in gas compounds CO_2, CH_4, and N_2 (Bakker and Jansen, 1990, 1994; Hall and Sterner, 1993). Also, salt concentrations in aqueous inclusions may show considerable changes during fluid inclusion modification (Hall and Wheeler, 1992). Secondary quartz and diffusional textures around fluid inclusions can be made visible in CL. In

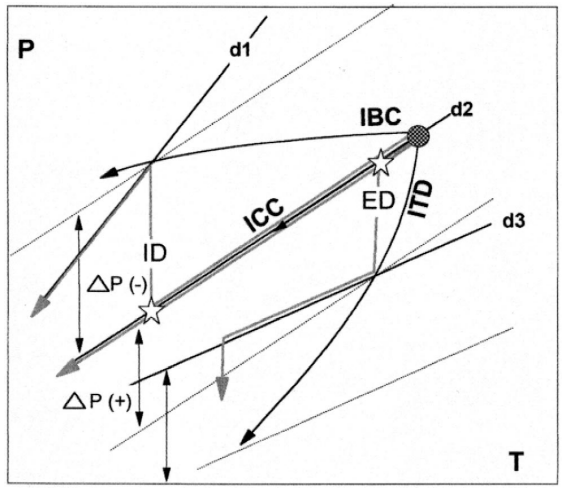

Fig. 10. The three principle regimes of fluid inclusion modification during retrograde conditions: on isobaric cooling (IBC), isochoric cooling (ICC), and isothermal decompression (ITD). Fluid inclusions may be modified due to the difference between fluid and confining pressure: fluid overpressure during uplift may result in explosion–decrepitation (ED), i.e. volume expansion, whereas fluid underpressure may result in implosion–decrepitation (ID), i.e. volume shrinkage. Fluid inclusions cooled along the isochore (d2), which cross-cuts the fluid trapping conditions, are largely preserved (see text for further explanation).

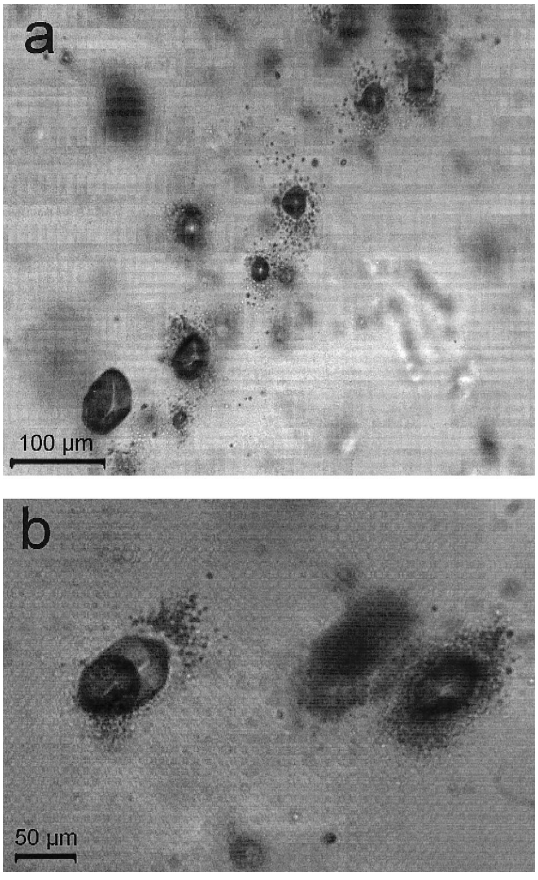

Fig. 11. Implosion–decrepitation textures: (a) modified fluid inclusions in Sn–W-bearing vein quartz are surrounded by small satellite inclusions (sample from Muhokore, Burundi, Hein et al., 1994a,b). Re-crystallization results in the reduction of the inclusion volume. (b) Detail of the same sample.

the paragraph below, we will discuss some applications of CL to fluid inclusion studies.

6. Principles of CL petrography

CL has become a routine and powerful study method in petrography (Marshall, 1988; Barker and Kopp, 1991). The technique involves the bombardment of a polished sample under vacuum by an electron beam that stimulates electron energy level transitions in the host mineral. The resulting photon emissions produce a luminescence of the mineral with variations in luminescence wavelength (color) and intensity being a complex function of trace element substitutions and defect structures. Two types of systems are available: simple and inexpensive microscope-mounted (cold cathode) systems which operate at relatively high gun currents and are principally of use for strongly luminescent phases such as carbonates and feldspars, or 'hot' (high-intensity) CL-microscopes (Zinkernagel, 1978; Ramseyer and Mullis, 1990; Neuser et al., 1995) which are much more sensitive to the relatively subdued luminescence of phases such as quartz. SEM-mounted CL detectors operate at lower currents and are particularly suitable for the study of microtextures on the scale of fluid inclusions (Boiron et al., 1992). Both optical and SEM–CL methods require carbon or gold coating of the sample. The coating could be probably obstructive for microthermometry and Raman analysis. Getting rid of this problem sometimes requires (slight) re-polishing of the sample.

A word of warning on the use of CL petrography is the possible damaging effect it may have on the fluid inclusion integrity. The high gun currents associated with cold cathode systems result in significant heating of the sample causing browning of resin or glues used in polished thin section preparation. Carbonate-hosted inclusions are often observed to leak under the beam, indicating that significant local heating occurs. Inclusions in stronger minerals such as quartz may be resistant; however, as a general rule, measuring fluid inclusions in samples after they have been used for CL studies is not recommended. The low gun currents associated with SEM–CL are, in contrast, not thought to result in any significant heating of the sample and tests on quartz-hosted inclusions have shown no modification of the microthermometry properties as a result of exposure under the SEM beam.

7. Evidence for fluid–rock interaction from quartz textures in CL

Quartz is not only the most studied mineral in relation to fluid inclusions, but also shows a highly variable and complex CL behavior due to the wide variety of possible defects in the quartz crystal struc-

ture. The CL of quartz is basically caused by point defect structures which in part are related with trace elements in the crystal lattice and in part are 'intrinsic' (Habermann et al., 1999). Trace elements may function as activator elements and show characteristic lines in the CL emission spectrum, e.g. Al (2.68–2.79 eV, blue), Ti (2.92–2.99 eV, blue), and Fe^{3+} (1.70–1.73 eV, red) (Perny et al., 1992; Stevens-Kalceff and Phillips, 1995; Van den Kerkhof et al., 1996; Van den Kerkhof and Müller, 1999a,b). A number of intrinsic CL emission lines occur and interfere with the other lines. Of particular interest for the study of fluid–quartz interaction are OH-related defect centers, which can be correlated with CL-emissions at 1.94–1.97 eV (orange/red). The state of water in minerals is various and may occur as crystal-bound water (defect structures, dislocations), micropores, pore water, water in microcracks, and last but not least in fluid inclusions. Geological processes may cause water to transform from one state into the other. For example, during prograde mineral reactions, water may be released by the breakdown of hydrous minerals and concentrate in fluid inclusions, whereas during retrograde metamorphism, water may be consumed to form hydrous minerals.

By optical CL-microscopy of quartz from Au-mineralized veins from Burundi (Hein et al., 1994a,b), it was possible to distinguish between two types of Au-bearing quartz veins showing dominant blue and red CL (Fig. 12a). The veins are dated 970 and 640 Ma, respectively. The quartz with blue CL contains fluid inclusions of 5–25 wt.% NaCl-equivalent and Th up to 320°C, whereas the quartz showing red luminescence (formed at lower temperature) contains fluid inclusions of lower salt concentration (0–5 wt.% NaCl-equivalent) and showing Th below 205°C. In this way, CL can be used to group fluid inclusion populations based on the relative age of the host quartz.

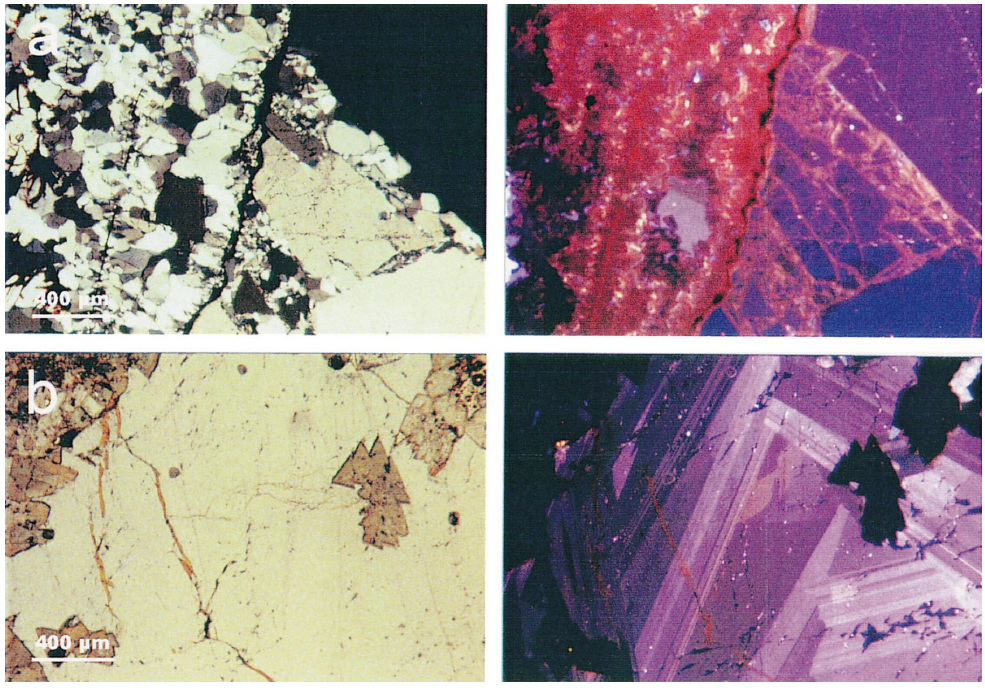

Fig. 12. Au-bearing quartz vein from Burundi (Hein et al., 1994a,b). (a) Two quartz generations show dominant blue and red CL (right image). The left image shows the same frame in transmitted light (crossed nicols). (b) The earliest Au-bearing quartz vein contains tourmaline (no CL) and shows clear growth zonation in CL (right image). Fluid inclusions are related with re-crystallized secondary quartz visible as dark patches in CL (lower right), but not in transmitted light (left image).

Primary CL textures in quartz essentially represent stages of growth zonation (Figs. 12b and 13a) and is often observed in non-deformed quartz. A direct correlation between fluid inclusions and growth zones may indicate their primary character. Fig. 13a shows an example of fluid inclusions

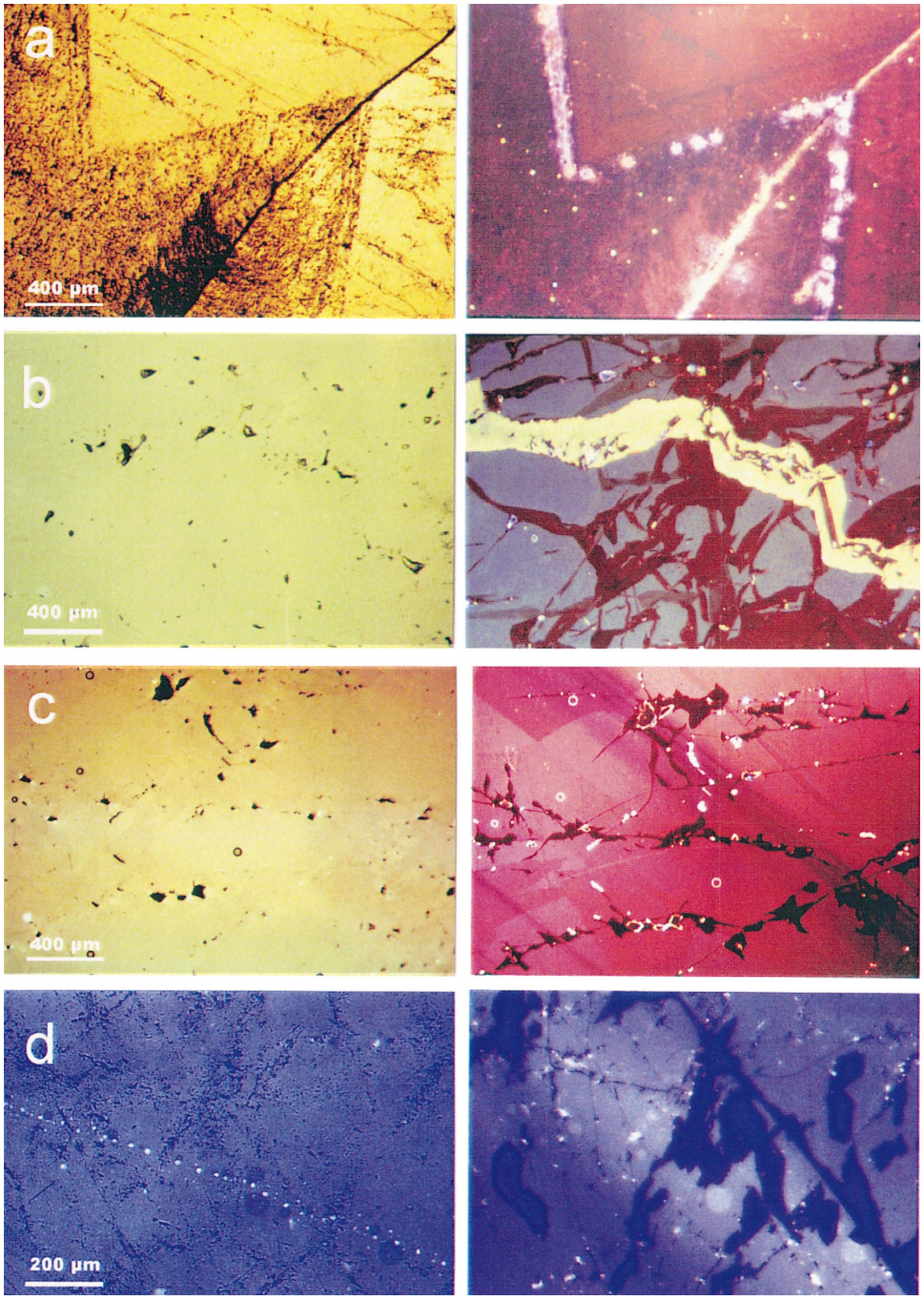

trapped during crystal growth. During one stage of crystal growth, highly saline fluid inclusions together with U-mineral inclusions were trapped and caused radiation damage of the surrounding quartz (bright CL).

Although primary textures are found in samples from different geological environment, the majority of microtextures visible in CL are of *secondary* character and formed during retrograde uplift. Fig. 13b shows secondary fluid inclusions trapped in a quartz veinlet formed in a single quartz crystal. In this way, secondary inclusions can be clearly distinguished from primary ones in the host crystal. The fact that CL is a surface effect (effecting 5 μm depth at maximum), whereas fluid inclusions (except for the ones outcropping at the surface and normally destroyed) occur at deeper levels in the sample. As a consequence, the direct combination of fluid inclusion (microthermometry) and CL data are basically impossible. Nevertheless, by estimating the three-dimensional extension of the textures, the information obtained by CL can be successfully used for the interpretation of fluid inclusions at depth in the sample.

Processes of fluid–rock interaction generally result in a local redistribution of trace elements (mainly Al, Li, Ti, Fe) and therewith also effect the CL properties. In different rock types, the similarity of the secondary microtextures related with fluid inclusions is remarkable. This indicates that most of these textures are the result of retrograde processes, which acted more or less along the same geothermal gradient.

A wide variety of CL textures related to fluid activity (mostly during retrograde conditions) has been observed since the late 1980s (Behr, 1989; Frentzel-Beyme, 1989). Recent studies (Van den Kerkhof and Müller, 1999a,b) show that *quartz healing* induced by fluid inclusions is a common cause for the CL textures, besides processes which result in the increase of the concentration of defect structures in the quartz crystal lattice. Fig. 13c–d shows examples of non-luminescent secondary quartz (with low trace element content compared to the host quartz) formed around fluid inclusions. The textures show that fluid inclusions largely control local fracturing and quartz re-crystallization. Healed microcracks typically connect fluid inclusions and indicate massive 'cascade-like' decrepitation. Trace elements are expelled from the re-crystallized parts and concentrate in the host quartz and/or in the fluid inclusions, which function as a sink for the released metal ions.

Microtextures are best studied by SEM–CL. They normally form as a result of fluid–rock interaction (alteration textures) and can be subdivided into two categories.

(1) Microtextures indicative of local lower crystal order (increasing the density of defect structures): micropores, dislocations, microfractures, grain boundary alteration (Fig. 14a).

(2) Microtextures indicative of quartz healing, i.e. the reduction of defect structures: secondary quartz formed by re-crystallization and quartz dissolution–precipitation. Secondary quartz is typically recognized as dark patchy halos around fluid inclusions (Fig. 14d). Healing textures include also secondary quartz fillings in which retrograde fluids are trapped. Fig. 14c shows a migmatite from Rogaland (Norway) containing retrograde fluid inclusions of CO_2–CH_4–H_2O–graphite composition and trapped below 400°C (Van den Kerkhof et al., 1991). The CL image shows that the inclusions are trapped along planes, which are largely controlled by lattice-controlled fracturing and formed as the result of pressure relaxation during uplift.

Fig. 13. Microtextures related with fluid inclusions in transmitted light (left) and in CL (right). (a) Primary fluid inclusions in quartz (Uranium deposit Großschloppen, Fichtelgebirge, Oberpfalz, Germany; Reutel, 1992). Complex highly saline Ca–Na–K ± Li fluid inclusions are trapped within one growth zone together with U-bearing mineral inclusions (autunite?). (b) Hydrothermal quartz (Hakos, Namibia) showing secondary fluid inclusions trapped in a veinlet cross-cutting the host quartz. (c) Secondary fluid inclusions in U-bearing quartz from Wäldel (Oberpfalz, Germany) associated with secondary, re-crystallized and non-CL quartz (collection: Behr, IGDL, Göttingen). (d) Quartz from retrogradely altered quartz from granulite (Bamble, Southern Norway). The quartz shows two generations of healing textures: idiomorphic crystal nuclei consist of pure quartz (non-detected trace elements) and represent parts where fluid inclusions have been healed. Fluid inclusions occur along the fine microfractures and secondary quartz patches formed at a stage of brittle deformation at lower temperature.

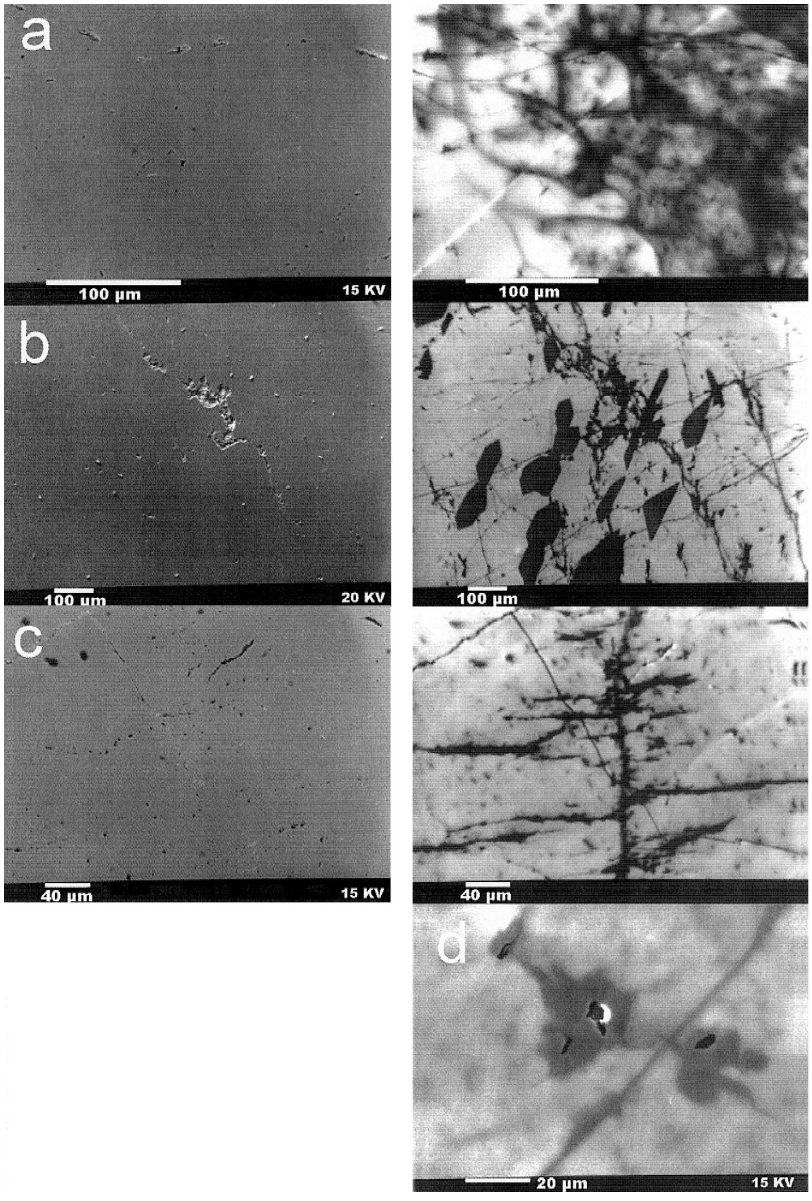

Fig. 14. SEM images in BSE and CL mode. (a) Granite near contact with intrusive enderbite (Natal, South Africa). Micropores in the originally 'wet' granite appear as black spots (right) and are largely healed in parts of the quartz, which are affected by the high-temperature event (desiccation). Fluid inclusions are found along late microfractures (Van den Kerkhof and Grantham, 1999) (b) Quartz from granulite (Bamble, Norway; cf. Fig. 13d). This detailed photograph clearly shows the time relations between earlier (high temperature) idiomorphic nuclei (pure quartz) and late healed fractures containing fluid inclusions. (c) Quartz from migmatite (Rogaland, Norway). Fluid inclusions in the sample contain CH_4–CO_2–H_2O and were trapped $< 400°C/2$ kbar (Van den Kerkhof et al., 1991). The median crack is parallel to crystallographic the *c*-axis. Fluid inclusions outcropping at the surface are visible in the BSE image. (d) Combined BSE/CL image of quartz in granite from Flössenburg (Oberpfalz, Germany). The inclusions (low salinity aqueous in the sample) are surrounded by re-crystallized pure quartz.

7.1. CL microtextures indicative of local lower crystal order

Micropores are characterized by dark (non-luminescent) 1–5 μm large spots and irregular lines, which become better visible after longer electron beam irradiation. In quartz with a high concentration of structural water like in granite this spotty texture is widespread (Van den Kerkhof and Grantham, 1999; Fig. 14a). The changes observed during electron beam irradiation may be indicative of the local transformation of crystal-bound water into molecular water, a mechanism assumed comparable with the results of Stenina et al. (1984) and Stenina (1995). Larger dislocations around fluid inclusions can be made visible by CL and assumed to be identical to the textures studied by TEM (Bakker and Jansen, 1990; Viti and Frezzotti, 2001). These dislocations are assumed to be the result of partial water leakage of the fluid inclusions. Alteration along grain boundaries normally appears in CL as diffuse dark zones and often decorates quartz grains and crystallites; similar textures have been observed around fluid inclusions and along larger cracks, which must have functioned as fluid pathways.

7.2. CL microtextures indicative of a local higher crystal order (healing)

As a result of quartz alteration, the trace element concentration around fluid inclusions and along grain boundaries is preferentially lowered. Whereas at higher temperatures diffusion by the induction of dislocations (hydrolytic weakening) is the main controlling process, at lower temperatures ($< 400°C$), brittle fracturing combined with quartz annealing by the formation of pure secondary quartz (precipitation–dissolution) is most important. These processes indicate the systematic recovery of defect structures and are possibly initiated by pressure gradients between fluid inclusion and host quartz. In this way, fluid inclusions function as nuclei for secondary quartz formation. The trace elements released from the purified quartz go into solution (fluid inclusions!) or react to form mineral inclusions, e.g. the formation of rutile needles in Ti-rich precursor quartz.

The processes for secondary quartz formation may be two-fold: on the one hand, defect structures in quartz immediately surrounding fluid inclusions may lose trace elements by diffusion and therefore, lower CL intensity. On the other hand, we find evidence for the formation of secondary quartz by dissolution–precipitation. At an advanced stage of recovery, new crystal faces may develop and replace a substantial part of the original quartz. The recovery of structural defects around fluid inclusions in extreme cases may even result in the complete disintegration of fluid inclusions. In quartz from enderbitic granulite from Bamble (Norway), we found evidence for two quartz healing episodes: one at higher temperature resulting in idiomorphic quartz nuclei and fluid inclusion recovery and another stage at lower temperatures resulting by ‘decrepitation’ of fluid inclusions at conditions of brittle deformation (Figs. 13d and 14b).

In spite of the problems of finding satisfying answers in interpreting the wide variety of fluid inclusion-related textures in quartz, we believe that CL-microscopy and the application of SEM–CL opens a way to better understand fluid–rock interaction processes and the formation of fluid inclusions.

8. Conclusion

The large variety of microtextures formed as a result of fluid–mineral interaction makes clear that a quick ‘routine’ study of fluid inclusions has hardly a realistic chance of drawing geologically relevant conclusions. This assertion is the more valid for the study of metamorphic rocks. We met different ways of describing fluid inclusions, based on external parameters like the shape (negative crystal, irregular, etc.) and internal parameters like the phase content at room temperature. The genetic classification, however, is most useful and principally indicates the relative time relations between the fluid inclusion and the host mineral as well as in between the different fluid inclusion generations (fluid chronology). Using different fluid inclusion classifications for single crystals and for massive rocks appeared to be plausible. By means of the so-called ‘trail classification’, information about the role of the fluid during deformation and/or re-crystallization can be obtained. In spite of the different fashionable terminol-

ogy (primary–secondary, early–late, etc.), we remind that any classification is always the means (workable or not) and not the aim of a study.

The recognition that fluid inclusions are not 'simple' cavities but an integral part of the mineral and that fluid inclusions are significant, but not the only witnesses of fluid–rock interaction processes (besides micropores, alteration rims, re-crystallization halos, etc.) makes CL highly valuable as an assisting method in 'fluid petrography'. By this method, fluid inclusion-related textures in quartz can be made visible. Not at all is the application of CL a condition of doing responsible studies on fluid inclusions and in many cases, careful microscopy is largely sufficient. In any case, the microstructural information obtained for single fluid inclusions or genetically related fluid inclusion groups is more important than investing time in producing large amounts of numerical data. It cannot be denied that the latter has been practiced for decades and certainly not by a minority of fluid inclusionists worldwide. Fluid inclusions should be given the significance, which was already recognized since the earliest days of fluid inclusion discovery in Sorby's time: an indispensable and above all, a fascinating part of petrology.

References

Anderson, A.J., Bodnar, R.J., 1993. An adaptation of the spindle stage for geometric analysis of fluid inclusions. Am. Mineral. 78, 657–664.

Audétat, A., Günther, D., 1999. Mobility and H_2O loss from fluid inclusions in natural quartz crystals. Contrib. Mineral. Petrol. 137, 1–14.

Bakker, R.J., Jansen, J.B.H., 1990. Preferential water leakage from fluid inclusions by means of mobile dislocations. Nature 345, 58–60.

Bakker, R.J., Jansen, J.B.H., 1994. A mechanism for preferential H_2O leakage from fluid inclusions in quartz, based on TEM observations. Contrib. Mineral. Petrol. 116, 7–20.

Barker, C.E., Kopp, O.C., 1991. Luminescence Microscopy and Spectroscopy: Qualitative and Quantitative Applications. Soc. of Economic Paleontologists and Mineralogists Short Course vol. 25, 195 pp.

Behr, H.J., 1989. Die geologische Aktivität von Krustenfluiden. Nds. Akad. Geowiss. Veröfftl. 1, 7–41.

Bethke, C.M., Marshak, S., 1990. Brine migrations across North America — the plate tectonics of groundwater. Annu. Rev. Earth Planet. Sci. Lett. 18, 287–315.

Bodnar, R.J., 1983. A method of calculating fluid inclusion volumes based on vapor bubble diameters and P–V–T–X properties of inclusion fluids. Econ. Geol. 78, 535–542.

Bodnar, R.J., Binns, P.R., Hall, D.L., 1989. Synthetic fluid inclusions — VI. Quantitative evaluation of the decrepitation behaviour of fluid inclusions in quartz at one atmosphere confining pressure. J. Metamorph. Geol. 7, 229–242.

Boiron, M.C., Essarraj, S., Sellier, E., Cathelineau, M., Lespinasse, M., Poty, B., 1992. Identification of fluid inclusions in relation to their host microstructural domains in quartz by cathodoluminescence. Geochim. Cosmochim. Acta 56, 175–185.

Coolen, J.J.M.M.M., 1982. Carbonic fluid inclusions in granulites from Tanzania — a comparison of geobarometric methods based on fluid density and mineral chemistry. Chem. Geol. 37, 59–77.

Frentzel-Beyme, K., 1989. REM-Kathodolumineszenz-Strukturen im Quarzteilgefüge von Metamorphiten: Bestandaufnahme und geologische Interpretation. PhD Dissertation, University of Göttingen, 77 pp.

Goldstein, R.H., 2001. Fluid inclusions in sedimentary and diagenetic systems. Lithos 55, 159–192 (this volume).

Habermann, D., Götze, J., Neuser, R.D., Richter, D.K., 1999. The phenomenon of intrinsic cathodoluminescence: case studies of quartz, calcite and apatite. Zentralbl. Geol. Palaeontol., Teil 1 H.10-12, 1275–1284.

Hall, D.L., Wheeler, J.R., 1992. Fluid composition and the decrepitation behavior of synthetic fluid inclusions in quartz. PACROFI IV Abstract Volume, Lake Arrowhead, California. p. 39.

Hall, D.L., Sterner, S.M., 1993. Preferential water loss from synthetic fluid inclusions. Contrib. Mineral. Petrol. 114, 489–500.

Hein, H.F., 1998. The bastnaesite–monazite deposits of Gakara/Burundi: composition of fluid inclusions and genetic implications. Freiberg. Forschungsh. C 475, 95–105.

Hein, U.F., Osswald, U., Behr, H.J., 1994a. Zur Charakterisierung erzbildender Lösungen mittels Fluideinschlußuntersuchungen: Unterkarbonische Eisenkiesel als Fallstudie für die exhalativ-sedimentäre Lagerstättenbildung. Berl. Geowiss. Abh., A 167, 197–204.

Hein, U.F., Behr, H.J., Van den Kerkhof, A.M., Osswald, U., Reutel, Chr., Schöttler, T., 1994b. Untersuchungen von Flüssigkeitseinschlüssen für die lagerstättengenetische Interpretation der Gold-Mineralisationen in NW-Burundi. Z. Angew. Geol. 40-2, 111.

Herms, P., Schenk, V., 1998. Fluid inclusions in high-pressure granulites of the Pan-African belt in Tanzania (Uluguru Mts.): a record of prograde to retrograde fluid evolution. Contrib. Mineral. Petrol. 130, 199–212.

Hurai, V., Horn, E.E., 1992. A boundary layer-induced immiscibility in naturally reequilibrated H_2O–CO_2–NaCl inclusions from metamorphic quartz (Western Carpathians, Czechoslovakia). Contrib. Mineral. Petrol. 112, 414–427.

Kooi, M.E., Schouten, J.A., Van den Kerkhof, A.M., Istrate, G., Althaus, E., 1998. The system CO_2–N_2 at high pressure and applications to fluid inclusions. Geochim. Cosmochim. Acta 62, 2837–2843.

Kranz, R.L., 1983. Micro-cracks in rocks: a review. Tectonophysics 100, 449–480.

Marshall, D.J., 1988. Cathodoluminescence of Geological Materials. Unwin Hyman, London, 146 pp.

Munz, I.A., 2001. Petroleum inclusions in sedimentary basins: systematics, analytical methods and applications. Lithos 55, 193–210 (this volume).

Neuser, R.D., Bruhn, F., Götze, J., Habermann, D., Richter, D.K., 1995. Kathodolumineszenz: Methodik und Anwendung. Zentralbl. Geol. Palaeontol., Teil 1 H.1/2, 287–306.

Perny, B., Eberhardt, P., Ramseyer, K., Mullis, J., Pankrath, R., 1992. Microdistribution of Al, Li, and Na in α-quartz: possible causes and correlation with short-lived cathodoluminescence. Am. Mineral. 77, 534–544.

Ramseyer, K., Mullis, J., 1990. Factors influencing short-lived blue cathodoluminescence of α-quartz. Am. Mineral. 75, 791–800.

Reutel, Chr., 1992. Krustenfluide in Gesteinen und Lagerstätten am Westrand der Böhmischen Masse. Göttinger Arb. Geol. Palaeontol. 53, 76 pp.

Roedder, E., 1979. Fluid inclusions as samples of ore fluids. In: Barnes, H.L. (Ed.), Geochemistry of Hydrothermal Ore Deposits. 2nd edn. Wiley, New York, pp. 684–737.

Roedder, E., 1984. Fluid inclusions, Reviews in Mineralogy vol. 12, Mineral. Soc. Am., Washington.

Shepherd, T.J., Rankin, A.H., Alderton, D.H.M., 1985. A Practical Guide to Fluid Inclusion Studies. Blackie and Son, Glasgow, 239 pp.

Simmons, G., Richter, D., 1976. Micro-cracks in rock. In: Strens, R.G.J. (Ed.), The Physics and Chemistry of Minerals and Rocks. Wiley, New York, pp. 105–137.

Stenina, N.G., 1995. Energy aspect in the formation of granitic magma and ore deposits. In: Pasava, J., Kribek, B., Zak, K. (Eds.), Mineral Deposits: From the Origin to their Environmental Impacts. Balkema, Rotterdam, pp. 539–542.

Stenina, N.G., Bazarov, L.Sh., Shcherbakova, Mya., Mashkovtsev, R.I., 1984. Structural state and diffusion of impurities in natural quartz of different genesis. Phys. Chem. Miner. 10, 180–186.

Sterner, S.M., Bodnar, R.J., 1989. Synthetic fluid inclusions: VII. Reequilibration of fluid inclusions in quartz during laboratory simulated metamorphic burial and uplift. J. Metamorph. Geol. 7, 243–260.

Stevens-Kalceff, M.A., Phillips, M.R., 1995. Cathodoluminescence microcharacterization of the structure of quartz. Phys. Rev. B 52-5, 3122–3134.

Touret, J.L.R., 1981. Fluid inclusions in high-grade metamorphic rocks. In: Hollister, L.S., Crawford, M.L. (Eds.), Short Course in Fluid Inclusions: Applications to Petrology. Mineralogical Association of Canada Short Course Handbook vol. 6, pp. 182–208.

Touret, J.L.R., 2001. Fluid inclusions in metamorphic rocks. Lithos 55, 1–25 (this volume).

Van den Kerkhof, A.M., Grantham, G.H., 1999. Metamorphic charnockite in contact aureoles around intrusive enderbite from Natal, South Africa. Contrib. Mineral. Petrol. 137, 115–132.

Van den Kerkhof, A.M., Müller, A., 1999a. Retrograde trace element redistribution in quartz and fluid inclusion modification: observations by cathodoluminescence. Abstract MinWien99, Berichte der DMG, Beihefte zum Eur. J. Mineral. 11, 121.

Van den Kerkhof, A.M., Müller, A., 1999b. Retrograde trace element redistribution in quartz and fluid inclusion modification: observations by cathodoluminescence. Berichte der Deutschen Mineralogischen Gesellschaft. Beih. z. Eur. J. Mineral. 11-1, 121.

Van den Kerkhof, A.M., Touret, J.L.R., Kreulen, R., 1994. Juvenile CO_2 in enderbites of Tromoy near Arendal, southern Norway: a fluid inclusion and stable isotope study. J. Metamorph. Geol. 12, 301–310.

Van den Kerkhof, A.M., Scherer, T., Riganti, A., 1996. Cathodoluminescence of Archean quartzites from the Nondweni Greenstone Belt, South Africa. Abstracts International Conference on Cathodoluminescence (SLMS), Nancy, France.

Van den Kerkhof, A.M., Touret, J.L.R., Maijer, C., Jansen, J.B.H., 1991. Retrograde methane-dominated fluid inclusions from high-temperature granulites of Rogaland, southwestern Norway. Geochim. Cosmochim. Acta 55, 2533–2544.

Viti, C., Frezzotti, M.-L., 2001. Transmission electron microscopy applied to fluid inclusion investigations. Lithos 55, 125–138 (this volume).

Vityk, M.O., Bodnar, R.J., 1995a. Textural evolution of synthetic fluid inclusions in quartz during reequilibration, with applications to tectonic reconstruction. Contrib. Mineral. Petrol. 121, 309–323.

Vityk, M.O., Bodnar, R.J., 1995b. Do fluid inclusions in high-grade metamorphic terranes preserve peak metamorphic density during retrograde decompression? Am. Mineral. 80, 641–644.

Vollbrecht, A., 1989. Mikroriß-Analyse im KTB — Datenerhebung U-Tisch Mikroskopie. Unpublished report IGDL, Göttingen.

Voznyak, D.K., Kalyuzhniy, V.A., 1976. Utilization of decrepitated inclusions for reconstruction of PT conditions of mineral formation on example of pegmatitic quartz from Volyn (in Russian). Miner. Sbornik 30, 31–40.

Zinkernagel, U., 1978. Cathodoluminescence of quartz and its application to sandstone petrology. Contributions to Sedimentology vol. 8, Schweizerbart'sche Verlagsbuchhandlung.